



Contents lists available at ScienceDirect

Mutation Research/Genetic Toxicology and Environmental Mutagenesis

journal homepage: www.elsevier.com/locate/gen tox
Community address: www.elsevier.com/locate/mutres



The reconstructed skin micronucleus assay in EpiDerm™: Reduction of false-positive results – a mechanistic study with epigallocatechin gallate



Katsuyuki Yuki, Naohiro Ikeda, Naohiro Nishiyama, Toshio Kasamatsu*

R&D-Safety Science Research, Kao Corporation, 2606 Akabane, Ichikai-Machi, Haga-Gun, Tochigi 321-3497, Japan

ARTICLE INFO

Article history:

Received 7 January 2013

Received in revised form 26 July 2013

Accepted 6 August 2013

Available online 27 August 2013

Keywords:

Reconstructed human skin model
Normal human epidermal keratinocytes
Micronucleus assay
Epigallocatechin gallate
False-positive
Reactive oxygen species

ABSTRACT

The high rate of false-positive or misleading results in in vitro mammalian genotoxicity testing is a hurdle in the development of valuable chemicals, especially those used in cosmetics, for which in vivo testing is banned in the European Union. The reconstructed skin micronucleus (RSMN) assay in EpiDerm™ (MatTek Corporation, USA) has shown promise as a follow-up for positive in vitro mammalian genotoxicity tests. However, few studies have explored its better predictive performance compared with existing in vitro assays. In the present study, we followed the protocol of the RSMN assay and used eight chemicals to compare micronucleus (MN) induction with EpiDerm™ with that in normal human epidermal keratinocytes (NHEKs), both derived from human skin. The assessments of EpiDerm™ conformed to those of in vivo MN assay, whereas those of NHEKs did not. The effect of cell differentiation status on MN induction was further addressed using a model compound, epigallocatechin gallate (EGCG), which is a major component of green tea extract that shows positive results in in vitro mammalian genotoxicity assays via oxidative stress and negative results in in vivo MN studies. RSMN assay in an underdeveloped epidermal model, EpiDerm-201™ (MatTek Corporation), showed a negative result identical to that in EpiDerm™, indicating that the barrier function of keratinocytes has limited impact. Analysis of the gene expression profile of both EpiDerm™ and NHEKs after EGCG treatment for 12 h revealed that the expression of genes related to genotoxic response was significantly induced only in NHEKs. Conversely, antioxidant enzyme activities (catalase and glutathione peroxidase) in EpiDerm™ were higher than those in NHEKs. These results indicate that EpiDerm™ has antioxidant properties similar to those of a living body and is capable of eliminating oxidative stress that may be caused by EGCG under in vitro experimental conditions.

© 2013 Elsevier B.V. All rights reserved.

1. Introduction

In vitro genotoxicity tests using mammalian cells are central to assessing the genotoxicity of chemicals, especially their capacity to damage chromosomes. However, these tests give high rates of false-positive (or misleading) results that are not confirmed by in vivo genotoxicity or carcinogenicity studies [1]. The false-positive rates in in vitro chromosomal aberration tests and micronucleus (MN) tests have been reported to be 55.1% and 59.2%, respectively [2]. Furthermore, 75–95% of rodent non-carcinogens give positive results in 1 or more in vitro genotoxicity tests [3]. Thus, conclusions drawn solely from results of in vitro genotoxicity tests are hurdles in the development of valuable

chemicals, especially those intended for use in cosmetics, for which follow-up in vivo testing is banned in the European Union.

Recently, a reconstructed skin micronucleus (RSMN) assay in EpiDerm™ (MatTek Corporation, Ashland, MA, USA) has been developed as a follow-up for positive in vitro results, especially for dermally applied chemicals, and it has demonstrated favorable predictive performance compared with in vivo genotoxicity tests [4–9]. The European Cosmetic Toiletry and Perfumery Association (currently Cosmetic Europe) has initiated a multi-laboratory international validation project for the RSMN assay with contributions from the European Centre for the Validation of Alternative Methods and has made solid progress [1].

EpiDerm™ consists of normal human epidermal keratinocytes (NHEKs) cultured to form a multilayered, highly differentiated model of the human epidermis (<http://www.mattek.com> [accessed April 7, 2013]). Structurally, EpiDerm™ consists of organized basal, spinous, granular, and cornified layers similar to those of human skin. Physiologically, EpiDerm™ is also mitotically and

* Corresponding author. Tel.: +81 285 68 7447; fax: +81 285 68 7452.
E-mail address: kasamatsu.toshio@kao.co.jp (T. Kasamatsu).

metabolically active [9–11]. Few studies have investigated the contribution of these characteristics to the better predictivity of the RSMN assay.

In the present study, we followed the protocol of the RSMN assay to compare MN induction responses in cells using EpiDerm™ and NHEKs. We used eight chemicals for which in vitro and in vivo genotoxicity data are available. We further addressed the structural and physiological advantages of EpiDerm™ related to predictive performance using a model compound, epigallocatechin gallate (EGCG). EGCG is a major component of green tea extract that gives positive results in in vitro mammalian genotoxicity assays via oxidative stress [12] and negative results in in vivo MN studies. Because the EpiDerm™ system is a multilayered skin model with barrier function, we were concerned that EGCG might not reach the target cells for evaluation, giving a negative result. We, therefore, analyzed EGCG in the medium underneath the target cells 24 h after the application of EGCG to the surface of the EpiDerm™ system. We then evaluated the effect of the barrier function of keratinocytes on MN induction using an underdeveloped epidermal model, EpiDerm-201™ (MatTek Corporation). The culturing of EpiDerm-201™ is identical to that of standard EpiDerm™, except that the culture period is shortened by 3 days. The resulting EpiDerm-201™ tissue is, thus, less mature in terms of epidermal development, reducing the barrier function of the tissue (<http://www.mattek.com/pages/products/epiderm201/> [accessed April 7, 2013]). Gene and key enzyme expression profiles of both EpiDerm™ and NHEKs were compared after EGCG application to understand the differences in physiological responses in both models.

2. Material and methods

2.1. Chemicals

For in vitro MN assay (Table 1), mitomycin C (MMC) was purchased from Kyowa Hakko Kirin (Tokyo, Japan), EGCG was purchased from Funakoshi (Osaka, Japan), and curcumin was purchased from KANTO CHEMICAL (Tokyo, Japan). *N*-methylnitrosourea (MNU), *N*-ethylnitrosourea (ENU), 4-nitrophenol (4-NP), 2-ethyl-1,3-hexanediol (EHD), and resorcinol (RES) were purchased from Sigma Aldrich (St. Louis, MO, USA). These chemicals were dissolved in acetone for EpiDerm™ models and in dimethylsulfoxide (DMSO) for NHEKs and prepared just before use (see Table 1).

Cytochalasin B (Cyto-B) and acridine orange were purchased from WAKO CHEMICAL (Tokyo, Japan). Trypan blue and trypsin-ethylenediaminetetraacetic acid (EDTA) solution were purchased from Invitrogen (NY, USA). Methanol, acetic acid, DMSO, and chloroform were purchased from KANTO CHEMICAL.

2.2. Models

EpiDerm™ (indicating EPI-200, a standard epidermis tissue model, in this manuscript unless specified otherwise), EpiDerm-201™ (underdeveloped epidermis tissue model EPI-201), and new maintenance medium that includes keratinocyte growth factor (EPI-100-NMM) were purchased from MatTek Corporation (MA, USA, Fig. 1). These models were shipped from the supplier at room temperature and usually arrived at our laboratory 3 days later. After receipt, they were stored at 4 °C and used within 48 h. The cells were transferred to 6-well plates containing 1 mL EPI-100-NMM maintained at $5.0 \pm 1.0\%$ CO₂ and 37.0 ± 1.0 °C overnight before use in the in vitro MN test.

NHEKs derived from neonatal foreskin and culture medium (HuMedia-KG2) were purchased from KURABO (Osaka, Japan).

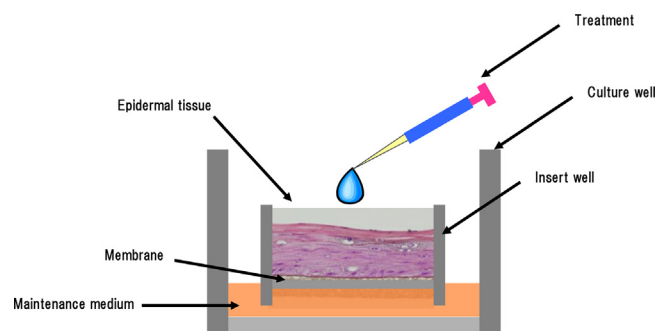


Fig. 1. Diagrammatic representation of EpiDerm™. The EpiDerm™ model (MatTek Corporation, USA) is derived from normal human epidermal keratinocytes (NHEKs) with differentiation from basal layer to horny layer. Maintenance medium is supplied to the basal layers through the membrane.

HuMedia-KG2 contained 0.4% bovine pituitary extract, 0.1% insulin, 0.1% human endothelial growth factor, 0.1% hydrocortisone, and 0.1% gentamicin and amphotericin mixture. NHEKs were seeded at 5.0×10^6 cells on the T175 dish with 15 mL of HuMedia-KG2 and used within passage 3.

2.3. In vitro MN assay

2.3.1. Assay in EpiDerm™ models (EPI-200 and EPI-201)

In vitro MN testing was carried out according to the method reported by Curren et al. [4]. Briefly, after pre-culture treatment overnight, the culture medium was replaced with 1 mL EPI-100-NMM containing 3 µg/mL Cyto-B, and 10 µL of each test chemical dissolved in acetone was applied to the surface of the models. The models were dosed twice at 24 h intervals and harvested 48 h after the first treatment. The culture medium was replaced concurrently with the dosing. The single-cell suspensions from the models were prepared through treatment with 0.25% trypsin-EDTA solution for 15 min. The cell suspension was centrifuged at 1000 rpm for 5 min and the supernatant was carefully removed. One milliliter of 0.075 M KCl solution was added to the cell pellet, mixed carefully, and kept at room temperature for 3 min. Three milliliters of cold methanol/acetic acid (3:1) was added to fix the cells, the cell suspension was centrifuged at 1000 rpm for 5 min, and the supernatant was removed. The fixation was repeated twice. The supernatant was removed, and the cell pellet was re-suspended in 200 µL methanol/acetic acid (99:1). Two drops of this cell suspension were pipetted onto the microscope slide. Three slides were prepared from each treatment and, after drying, stored at room temperature until observation.

Acridine orange solution (25 µg/mL) was applied to the slides to stain the cells, and the slides were scored using a fluorescence microscope (OLYMPUS BX51, Tokyo, Japan). More than 1000 binucleated cells (if possible) containing MNs were observed per slide (3000 binucleated cells per treatment), and the MN frequency was calculated. The outcome of the assay was considered positive when statistically significant ($P < 0.05$) MN induction was confirmed between solvent control and treatment using the 1-sided Fisher's exact test.

Current Organization for Economic Co-operation and Development guideline 487 recommends cytokinesis-block proliferation index determination for the evaluation of cytotoxicity when Cyto-B is used. Because we followed the protocol of Curren et al. [4], to compare to results reported previously [4,9], we assessed cytotoxicity by counting the relative binucleated cells compared to the solvent control. The average percentage of binucleated cells in EpiDerm™ was 75.9 ± 8.4 that of solvent (acetone) control throughout the present study (total, 15 tissues).

Table 1
Compounds tested.

| Chemical name | Abbreviation | CAS No. | Supplier | Purity (%) | In vitro CA* | In vivo MN** |
|-------------------------------|--------------|----------|-------------------|------------|--------------|--------------|
| Genotoxins | | | | | | |
| Mitomycin C | MMC | 50-07-7 | Kyowa Hakko Kirin | 99 | +++ | +(5) |
| N-methylnitrosourea | MNU | 684-93-5 | Sigma-Aldrich | >99 | +++ | +(5) |
| N-ethylnitrosourea | ENU | 759-73-9 | Sigma-Aldrich | >99 | +++ | +(5) |
| Non-in vivo genotoxins | | | | | | |
| 4-Nitrophenol | 4-NP | 100-02-7 | Sigma-Aldrich | >99 | +++ | —(5)**** |
| 2-Ethyl-1,3-hexanediol | EHD | 94-96-2 | Sigma-Aldrich | 97 | ++ | —(5)**** |
| Epigallocatechin gallate | EGCG | 989-51-5 | Funakoshi | >90 | +++ | —(9) |
| Curcumin | CRU | 458-37-7 | Kanto Chemical | >98 | +++ | —(2) |
| Resorcinol | RES | 108-46-3 | Sigma-Aldrich | >99 | +++ | —(2) |

* Chromosomal aberration test.

** Micronucleus test.

*** In-house unpublished data.

**** In vivo skin MN assay.

+: Positive; -: negative.

2.3.2. Assay in NHEKs

The NHEKs of passage 2 were collected and seeded at 1.0×10^5 cells on the 6-well plates with 2 mL HuMedia-KG2 per well. The next day, the culture medium was replaced with 1 mL HuMedia-KG2 containing both 0.1% test chemical solutions in DMSO, and the culture medium replacement was repeated after 24 h. No Cyto-B was applied to NHEKs. Forty-eight hours after the first treatment, the single-cell suspensions from the NHEKs were prepared through treatment with 0.25% trypsin-EDTA solution for 3 min. Part of the suspension was diluted with trypan blue solution to discriminate between the dead and living cells, and cytotoxicity was evaluated by counting live cells and comparing them with those of concurrent solvent controls (DMSO treatment). The fixation of the cells, preparation, and observation of specimens were carried out using the protocol for the EpiDerm™ model described above.

2.4. High-performance liquid chromatography analysis

EGCG concentration in the culture medium was analyzed according to the method reported by Lee et al. [13], with minor modification. All samples were analyzed using a high-performance

liquid chromatography system (Waters 2695 separation module, Milford, MA, USA) with an electrochemical detector, Coulochem III (ESA, Sunnyvale, CA, USA). An Inertsil ODS2 (4.6 mm \times 250 mm) column was used. The temperature of the column and guard column were maintained at 35 °C, and the autosampler was maintained at 6 °C. The flow rate was 1 mL/min, and the injection volume was 50 μ L per sample. For binary gradient elution, solution A was 100 mM sodium phosphate buffer containing 1.75% acetonitrile and 0.12% tetrahydrofuran at a final apparent pH of 3.35. Solution B was 15 mM sodium phosphate buffer containing 58.5% acetonitrile and 12.5% tetrahydrofuran at a final apparent pH of 3.45. The gradient program for the analysis of EGCG consisted of an initial 7-min isocratic segment (96% solution A and 4% solution B). The linear gradient was then changed progressively by increasing solution B to 17% at 25 min, 28% at 31 min, 33% at 37 min, and 98% at 38 min. It was maintained at 98% solution B from 38 to 43 min and finally changed back to 4% solution B from 44 to 55 min. The range of detection was 3 to 10,000 ng/mL. The eluent was monitored using the electrochemical detector with the potential set at –150 (E1), 300 (E2), and 350 (guard) mV. All data analysis was performed using Empower (Waters, Milford, PA, USA).

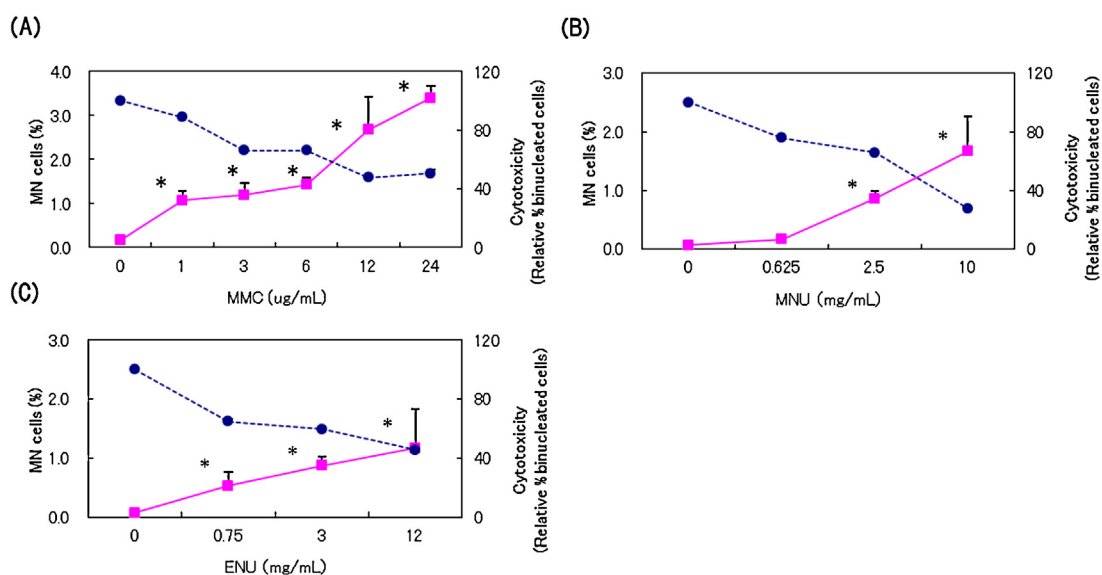


Fig. 2. Cytotoxicity and micronucleus (MN) induction in EpiDerm™ after treatment with known genotoxins. Solid lines indicate the percentage of binucleated cells with MNs (left axis); dashed lines indicate the percentage of cytotoxicity (right axis). Three tissues were evaluated at each dose. Error bars indicate standard deviation in the three tissues in the experiment. *Significant increase in MN induction compared to induction in the concurrent control ($P < 0.05$). (A) Mitomycin C (MMC); (B) *N*-methylnitrosourea (MNU); (C) *N*-ethylnitrosourea (ENU).

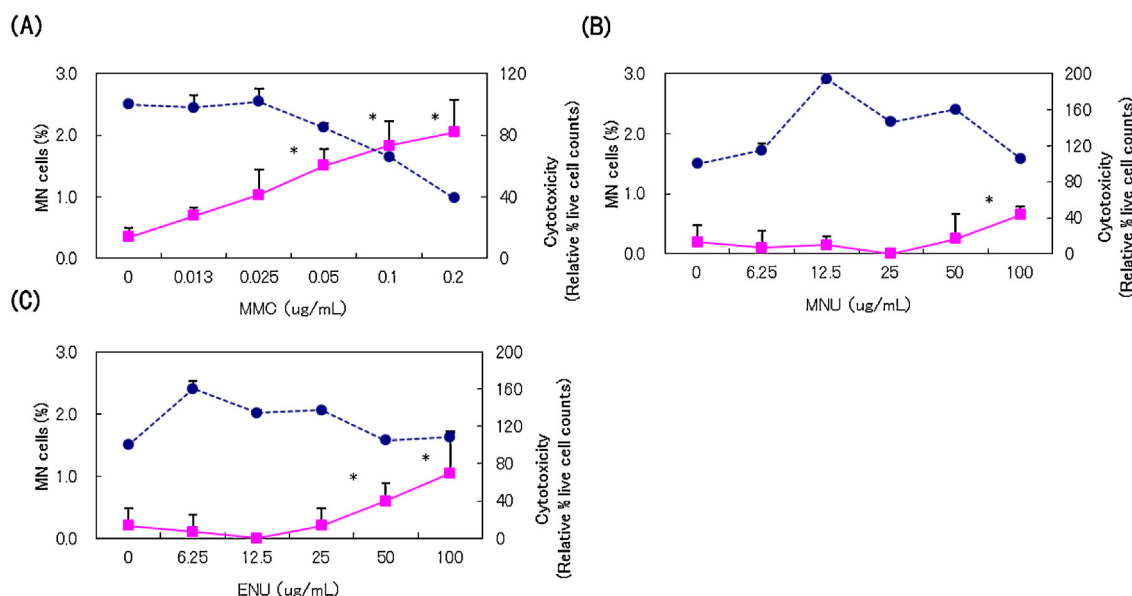


Fig. 3. Cytotoxicity and micronucleus (MN) induction in normal human epidermal keratinocytes after treatment with known genotoxins. Solid lines indicate the percentage of binucleated cells with MNs (left axis); dashed lines indicate the percentage of cytotoxicity (right axis). Three tissues were evaluated at each dose. Error bars indicate standard deviation in the three tissues in the experiment. *Significant increase in MN induction compared to induction in the concurrent control ($P < 0.05$). (A) Mitomycin C (MMC); (B) *N*-methylnitrosourea (MNU); (C) *N*-ethylnitrosourea (ENU).

2.5. RNA extraction

Total RNA was extracted from the EpiDermTM models using TRIzol reagent (Invitrogen, Carlsbad, CA, USA). After treatment with 10 mg/mL EGCG for 0, 1, 6, 12, and 24 h, all samples were homogenized with 1.0 mL TRIzol reagent, and 0.2 mL chloroform was added. The clear aqueous layer (containing RNA) was transferred to new RNase-free tubes after centrifugation at 15,000 rpm for 15 min at 4 °C. The aqueous layer was added to the same volume of isopropanol, mixed carefully, and centrifuged at 15,000 rpm for 10 min at 4 °C. The supernatant was removed, added to 1.0 mL 80% ethanol, and centrifuged at 15,000 rpm for 5 min at 4 °C. After the removal of the supernatant, the RNA pellet was dried at room temperature for 15 min, and 30 µL RNase-free water was added to dissolve the pellet at the bottom of the tube. The RNA solution was purified with a column using an RNeasy mini kit (Cat No. 74104) purchased from Qiagen (Tokyo, Japan). Total RNA from NHEKs was extracted and purified with a column using an RNeasy mini kit (Qiagen). The quality and concentration of total RNA were checked using a Nanodrop ND1000 spectrometer (LMS, Tokyo, Japan). The total RNA obtained was used for DNA microarray analysis and quantitative real-time polymerase chain reaction (RT-PCR) as described below.

2.6. DNA microarray analysis

DNA microarray analysis was performed using a GeneChip (Human Genome U133 Plus 2.0 Array, Affymetrix, Tokyo, Japan). Complementary DNA (cDNA) synthesis, complementary RNA (cRNA) labeling, and hybridization on the GeneChip were carried out at KURABO. Briefly, 250 ng total RNA was converted to cDNA. Biotin-labeled cRNAs were synthesized using an IVT Labeling Kit (Affymetrix), and prepared cRNA was hybridized to the GeneChip. cRNA was prepared in triplicate for each treatment. The gene expression data obtained through laser scanning of the hybridized chips was analyzed using GeneSpring (Ver. 11, Agilent Technologies, Tokyo, Japan) as follows. First, raw gene expression data were normalized using 1 of 3 corresponding controls (0 h treatment). Second, all data were classified into three flags – present, absent, and marginal – and only genes that had a present flag in triplicate

were selected. Changes in gene expression were determined by measuring the fold change (ratio) of mean values for signals in each group. Among gene probes showing a greater than 1.5-fold change in signal intensity between the EGCG treatment group at 12 h and the concurrent control (0 h), gene ontology (GO) analysis was performed to identify GO terms as biological processes with statistical significance ($P < 0.01$) using the 1-sided Fisher's exact test.

2.7. RT-PCR

RT-PCR was performed using an Applied Biosystems 7900 Fast Real-Time PCR System (Applied Biosystems, Foster City, CA, USA). The RT-PCR conditions were as follows: a 10-min hot start at 95 °C, followed by 40 cycles of 95 °C for 15 s and 60 °C for 1 min. cDNA was synthesized from 1 µg total RNA using SuperScript III reverse transcriptase (Cat No., 18080-051) purchased from Invitrogen. Expression levels of the following genes were analyzed using Taqman probe sets purchased from Applied Biosystems: catalase (*CAT*, *Hs00156308.m1*), glutathione peroxidase 1 (*Gpx1*, *Hs02516751.s1*), and glutamate-cysteine ligase, and catalytic subunit (*GCLC*, *Hs00155249.m1*). These data were corrected with expression data of an internal standard ribosomal protein, large, P0 (*RPLP0*, *Hs99999902.m1*).

2.8. Measurement of reactive oxygen species (ROS)

Intracellular ROS levels were measured using an ROS-specific probe, chloromethyl-H₂DCFDA (Cat No., C6827; Invitrogen). The probe was deacetylated inside the cell, and the subsequent oxidation by intracellular oxidants yielded a fluorescent product. EpiDermTM systems and NHEKs were treated with 10 mg/mL or 10 µg/mL EGCG, respectively, for 0, 1, 3, 6, and 12 h. After treatment, the cells were washed with phosphate-buffered saline (–) 3 times and incubated for 30 min at 37 °C with phosphate-buffered saline (–) containing 100 nM chloromethyl-H₂DCFDA. The cells were then collected, homogenized with a micro-homogenizer, and centrifuged at 10,000 rpm for 5 min at 4 °C. ROS levels in the supernatants were measured using a fluorescence plate-reader at 492–495/517–527 nm. Each fluorescent index was corrected per

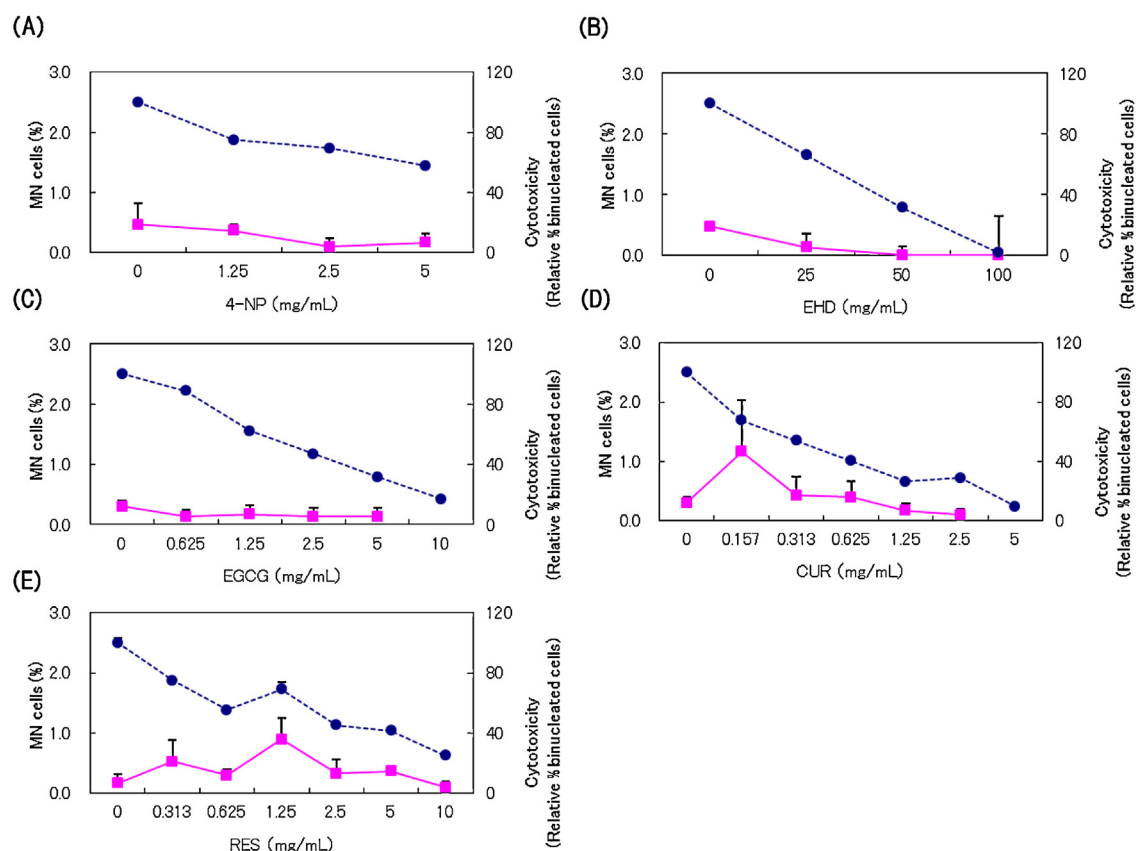


Fig. 4. Cytotoxicity and micronucleus (MN) induction in EpiDerm™ after treatment with non-in vivo genotoxins. Solid lines indicate the percentage of binucleated cells with MNs (left axis); dashed lines indicate the percentage of cytotoxicity (right axis). Three tissues were evaluated at each dose. Error bars indicate standard deviation in the three tissues in the experiment. *Significant increase in MN induction compared to induction in the concurrent control ($P < 0.05$). (A) 4-Nitrophenol (4-NP); (B) 2-ethyl-1,3-hexanediol (EHD); (C) epigallocatechin gallate (EGCG); (D) curcumin (CUR); (E) resorcinol (RES).

milligram protein. The protein content of each model was measured using a bicinchoninic acid protein assay kit (Cat No. 23227) purchased from Thermo Scientific (Rockford, IL, USA).

2.9. Antioxidant enzyme activity assays

CAT and GPx activities were measured using kits (Cat Nos. 707002 and 703102, respectively) purchased from Cayman Chemical (Ann Harbor, MI, USA). The EpiDerm™ (EPI-200 and EPI-201) systems and NHEKs were treated with 10 mg/mL or 10 μ g/mL of EGCG, respectively, for 0, 1, 3, 6, and 12 h. After treatment, the cells were collected from the insert by using tweezers and homogenized using a micro-homogenizer. These homogenates were centrifuged at 10,000 rpm for 5 min, and the supernatants were transferred to a new 96-well plate to measure CAT and GPx enzyme activities. The measurement of CAT activity was based on the reaction of the enzyme with methanol in the presence of an optimal concentration of H_2O_2 . The produced formaldehyde was measured with absorbance at 540 nm. One unit of CAT was defined as the formation of 1 nmol formaldehyde per minute per milligram of protein. GPx activity was measured indirectly using a coupled reaction with glutathione reductase. The oxidized form of glutathione, glutathione disulfide, produced by the reduction of hydroperoxides by GPx was recycled to its reduced form, glutathione, through the oxidation of NADPH to $NADP^+$, which was accompanied by a decrease in absorbance at 340 nm. Under the conditions of the assay, the rate of decrease in absorbance at 340 nm was directly proportional to the GPx activity in the sample. One unit of GPx was defined as

the amount of enzyme causing the oxidation of 1 nmol NADPH per minute per milligram of protein. The protein content of each model was measured as described above.

3. Results

3.1. Comparison of EpiDerm™ and NHEKs for MN induction

Table 1 lists the eight chemicals evaluated for their potential to induce MNs in EpiDerm™ and NHEKs. Following the RSMN assay protocol described by Curren et al. [4], we treated each cell system with test chemicals and determined the significance of MN induction.

In vivo genotoxins (MMC, MNU, and ENU) induced significant MNs in both EpiDerm™ (Fig. 2) and NHEKs (Fig. 3). Non-in vivo genotoxins (4-NP, EHD, EGCG, curcumin, and RES) caused no significant MN induction in EpiDerm™, although dose-dependent cytotoxicity was observed (Fig. 4). Furthermore, non-in vivo genotoxins, with the exception of RES, induced significant MNs in NHEKs (Fig. 5). Determinations of MN induction in EpiDerm™ conformed to those of in vivo MN assays, whereas NHEKs incorrectly identified three of four non-in vivo genotoxins evaluated.

Each experiment included a positive control (MMC at doses of 12 μ g/mL in EpiDerm™ and 0.1 μ g/mL in NHEKs) and confirmed significant MN induction (average % MN were 1.8 ± 0.6 in EpiDerm™ and 1.9 ± 0.4 in NHEKs). (The total number of tissues evaluated in both EpiDerm™ and NHEKs was 15.)

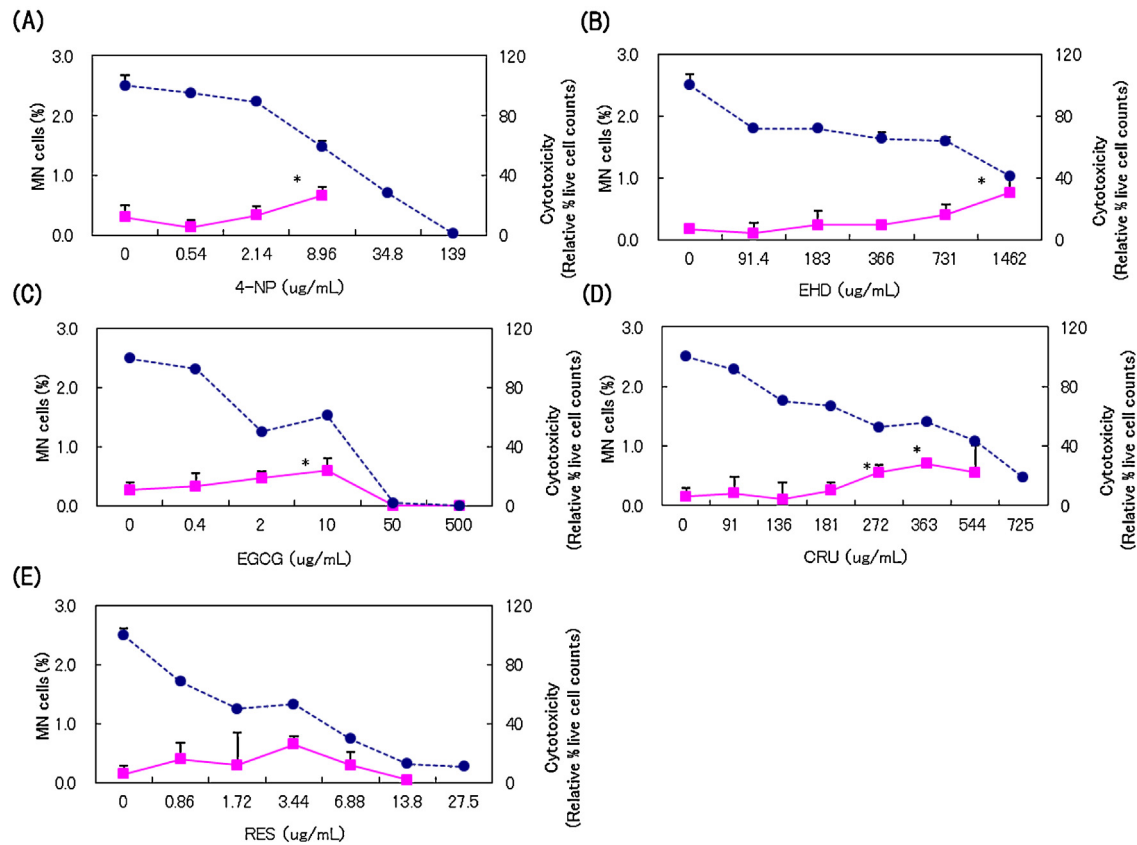


Fig. 5. Cytotoxicity and micronucleus (MN) induction in normal human epidermal keratinocytes after treatment with non-in vivo genotoxins. Solid lines indicate the percentage of binucleated cells with MNs (left axis); dashed lines indicate the percentage of cytotoxicity (right axis). Three tissues were evaluated at each dose. Error bars indicate standard deviation in the three tissues in the experiment. *Significant increase in MN induction compared to induction in the concurrent control ($P < 0.05$). (A) 4-Nitrophenol (4-NP); (B) 2-ethyl-1,3-hexanediol (EHD); (C) epigallocatechin gallate (EGCG); (D) curcumin (CUR); (E) resorcinol (RES).

3.2. Detection of EGCG in the medium beneath EpiDerm™ after topical application

Concentrations of EGCG in the medium were measured 24 h after EGCG application on the surface of EpiDerm™ at various doses (Fig. 6). EGCG was detected in the medium, and the concentration was increased in proportion to the doses applied, indicating that EGCG penetrated EpiDerm™ from the surface to reach the medium beneath the cells.

3.3. RSMN assay with EGCG in EpiDerm-201™

EpiDerm-201™ is an underdeveloped epidermal model that is 3 days younger than the standard EpiDerm™ model

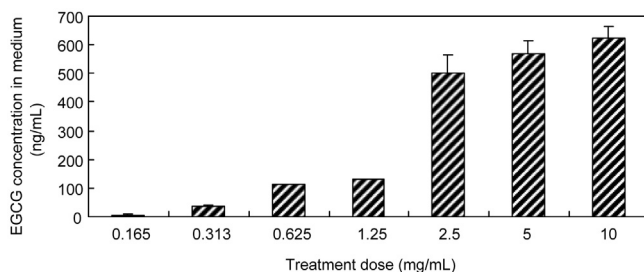


Fig. 6. Concentrations of epigallocatechin gallate (EGCG) in the culture medium of EpiDerm™ 24 h after application. EGCG was applied onto the surface of EpiDerm™ at various doses. Twenty-four hours after application, EGCG was detected in the medium, and the concentration was increased in proportion to the doses applied. Error bars indicate standard deviation in three tissues at each dose.

(EPI-200) and has a partially cornified epidermal structure (<http://www.mattek.com> [accessed April 7, 2013]). RSMN assay in EpiDerm-201™ treated with EGCG gave a negative result (Fig. 7) that agreed with the results in EpiDerm™. The positive control (MMC at a dose of 12 µg/mL) showed significant MN induction ($3.3 \pm 1.0\%$ in three tissues) compared to the solvent control ($0.1 \pm 0.2\%$ in three tissues). Average percentage of binucleated cells in the positive control and solvent control were 51.2 ± 1.4 and 55.7 ± 4.3 , respectively.

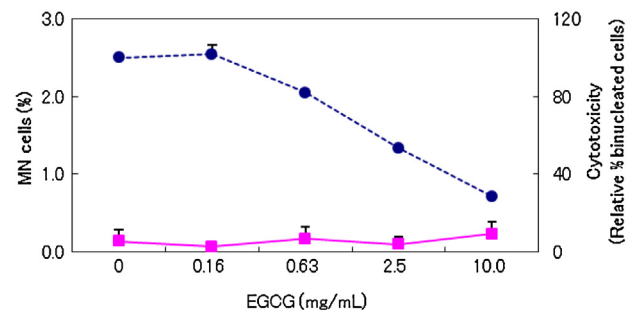


Fig. 7. Cytotoxicity and micronucleus (MN) induction in EpiDerm-201™ treated with epigallocatechin gallate (EGCG). Solid line indicates the percentage of binucleated cells with MN (left axis); dashed line indicates the percentage of cytotoxicity (right axis). Three tissues were evaluated at each dose. Error bars indicate standard deviation in the three tissues in the experiment. *Significant increase in MN induction compared to induction in the concurrent control ($P < 0.05$).

Table 2
Gene ontology (GO) biological processes altered in EpiDerm™.

| GO accession | GO term | P value |
|--------------|--|----------|
| GO:0048513 | Organ development | 4.60E–09 |
| GO:0048856 | Anatomical structure development | 5.24E–09 |
| GO:0048731 | System development | 5.66E–09 |
| GO:0022402 | Cell cycle process | 8.94E–09 |
| GO:0005856 | Cytoskeleton | 1.44E–08 |
| GO:0007049 | Cell cycle | 2.72E–08 |
| GO:0008544 | Epidermis development | 6.94E–08 |
| GO:0032502 | Developmental process | 1.24E–07 |
| GO:0000278 | Mitotic cell cycle | 1.36E–07 |
| GO:0022403 | Cell cycle phase | 1.94E–07 |
| GO:0000087 | M phase of mitotic cell cycle | 5.07E–07 |
| GO:0007275 | Multicellular organismal development | 7.29E–07 |
| GO:0007067 | Mitosis | 7.73E–07 |
| GO:0000280 | Nuclear division | 7.73E–07 |
| GO:0003824 | Catalytic activity | 8.46E–07 |
| GO:0015630 | Microtubule cytoskeleton | 9.36E–07 |
| GO:0007398 | Ectoderm development | 1.44E–06 |
| GO:0044430 | Cytoskeletal part | 1.55E–06 |
| GO:0048285 | Organelle fission | 2.17E–06 |
| GO:0044255 | Cellular lipid metabolic process | 2.18E–06 |
| GO:0048646 | Anatomical structure formation involved in morphogenesis | 3.86E–06 |

GO analysis was performed using GeneSpring (Ver. 11, Agilent Technologies, Tokyo, Japan). The GO terms shown were altered by 12-h epigallocatechin gallate treatment (10 mg/mL) and ranked according to *P* value. Expression of 2391 genes was up- or down-regulated (>1.5-fold change), and 21 biological processes were identified with statistical significance ($P < 0.01$) using Fisher's exact test.

Table 3
Gene ontology (GO) biological processes altered in normal human epidermal keratinocytes.

| GO accession | GO term | P value |
|--------------|---|----------|
| GO:0005622 | Intracellular | 3.78E–41 |
| GO:0044424 | Intracellular part | 2.96E–38 |
| GO:0043227 | Membrane-bounded organelle | 3.93E–32 |
| GO:0043231 | Intracellular membrane-bounded organelle | 5.09E–31 |
| GO:0043226 | Organelle | 5.02E–25 |
| GO:0043229 | Intracellular organelle | 5.67E–25 |
| GO:0005737 | Cytoplasm | 9.26E–24 |
| GO:0003824 | Catalytic activity | 3.48E–18 |
| GO:0044446 | Intracellular organelle part | 3.29E–16 |
| GO:0044422 | Organelle part | 5.54E–16 |
| GO:0005634 | Nucleus | 9.20E–16 |
| GO:0006259 | DNA metabolic process | 1.43E–15 |
| GO:0006974 | Response to DNA damage stimulus | 1.89E–15 |
| GO:0044428 | Nuclear part | 3.29E–15 |
| GO:0034984 | Cellular response to DNA damage stimulus | 1.66E–13 |
| GO:0008152 | Metabolic process | 2.06E–13 |
| GO:0044238 | Primary metabolic process | 3.13E–13 |
| GO:0006260 | DNA replication | 5.39E–13 |
| GO:0006281 | DNA repair | 7.37E–13 |
| GO:0007049 | Cell cycle | 2.16E–11 |
| GO:0044237 | Cellular metabolic process | 5.74E–11 |
| GO:0006807 | Nitrogen compound metabolic process | 6.23E–11 |
| GO:0033554 | Cellular response to stress | 7.83E–11 |
| GO:0031974 | Membrane-enclosed lumen | 8.60E–11 |
| GO:0031981 | Nuclear lumen | 1.47E–10 |
| GO:0005654 | Nucleoplasm | 1.82E–10 |
| GO:0070013 | Intracellular organelle lumen | 3.45E–10 |
| GO:0044444 | Cytoplasmic part | 6.10E–10 |
| GO:0043233 | Organelle lumen | 1.06E–09 |
| GO:0022403 | Cell cycle phase | 5.55E–09 |
| GO:0006139 | Nucleobase, nucleoside, nucleotide and nucleic acid metabolic process | 7.14E–09 |
| GO:0016740 | Transferase activity | 9.04E–09 |
| GO:0012505 | Endomembrane system | 9.45E–09 |
| GO:0043412 | Macromolecule modification | 3.26E–08 |
| GO:0017076 | Purine nucleotide binding | 4.39E–08 |
| GO:0022402 | Cell cycle process | 5.77E–08 |
| GO:0000279 | M phase | 5.95E–08 |
| GO:0000087 | M phase of mitotic cell cycle | 6.11E–08 |

Table 3 (Continued)

| GO accession | GO term | P value |
|-----------------------|--|----------|
| GO:0031090 | Organelle membrane | 6.92E–08 |
| GO:0007067 | Mitosis | 1.10E–07 |
| GO:0000280 | Nuclear division | 1.10E–07 |
| GO:0000166 | Nucleotide binding | 1.14E–07 |
| GO:0051716 | Cellular response to stimulus | 1.31E–07 |
| GO:0016879 | Ligase activity, forming carbon-nitrogen bonds | 1.32E–07 |
| GO:0046907 | Intracellular transport | 1.52E–07 |
| GO:0016874 | Ligase activity | 1.53E–07 |
| GO:0006464 | Protein modification process | 1.60E–07 |
| GO:0044260;GO:0034960 | Cellular macromolecule metabolic process | 2.21E–07 |
| GO:0043122 | Regulation of I-kappaB kinase/nuclear factor-kappaB cascade | 2.27E–07 |
| GO:0043123 | Positive regulation of I-kappaB kinase/nuclear factor-kappaB cascade | 3.80E–07 |
| GO:0048285 | Organelle fission | 4.14E–07 |
| GO:0000075 | Cell cycle checkpoint | 4.76E–07 |
| GO:0004386 | Helicase activity | 5.13E–07 |
| GO:0034613;GO:0016249 | Cellular protein localization | 5.33E–07 |
| GO:0044248 | Cellular catabolic process | 5.57E–07 |
| GO:0070727 | Cellular macromolecule localization | 5.68E–07 |
| GO:0010740 | Positive regulation of protein kinase cascade | 6.11E–07 |
| GO:0006886 | Intracellular protein transport | 6.80E–07 |
| GO:0006996 | Organelle organization | 1.04E–06 |
| GO:0044464 | Cell part | 1.69E–06 |
| GO:0005623 | Cell | 1.81E–06 |
| GO:0015031;GO:0015831 | Protein transport | 1.91E–06 |
| GO:0006605 | Protein targeting | 2.28E–06 |
| GO:0017111 | Nucleoside-triphosphatase activity | 2.52E–06 |
| GO:0016070 | RNA metabolic process | 2.99E–06 |
| GO:0006396;GO:0006394 | RNA processing | 3.15E–06 |
| GO:0045184 | Establishment of protein localization | 3.24E–06 |
| GO:0051301 | Cell division | 3.25E–06 |
| GO:0016881 | Acid-amino acid ligase activity | 3.42E–06 |
| GO:0005515;GO:0045308 | Protein binding | 3.88E–06 |
| GO:0000278 | Mitotic cell cycle | 4.23E–06 |
| GO:0016818 | Hydrolase activity, acting on acid anhydrides, in phosphorus-containing anhydrides | 4.32E–06 |
| GO:0005657 | Replication fork | 5.09E–06 |
| GO:0001882 | Nucleoside binding | 5.31E–06 |
| GO:0044265;GO:0034962 | Cellular macromolecule catabolic process | 5.55E–06 |
| GO:0005783 | Endoplasmic reticulum | 5.59E–06 |
| GO:0008104 | Protein localization | 5.89E–06 |
| GO:0016462 | Pyrophosphatase activity | 6.01E–06 |
| GO:0016043 | Cellular component organization | 6.52E–06 |
| GO:0016817 | Hydrolase activity, acting on acid anhydrides | 8.11E–06 |
| GO:0015630 | Microtubule cytoskeleton | 9.21E–06 |
| GO:0004518 | Nuclease activity | 9.49E–06 |
| GO:0010627 | Regulation of protein kinase cascade | 1.01E–05 |
| GO:0004527 | Exonuclease activity | 1.07E–05 |

GO analysis was performed using GeneSpring (Ver. 11, Agilent Technologies). GO terms shown were altered by 12-h epigallocatechin gallate treatment (10 µg/mL) and ranked according to *P* value. GO terms related to genotoxicity are shaded. Expression of 3944 genes was up- or down-regulated (>1.5-fold change), and 84 biological processes were identified with statistical significance ($P < 0.01$) using Fisher's exact test.

3.4. Comparison of gene expression profiles in EpiDerm™ and NHEKs after EGCG treatment

To understand the differences in biological processes or pathways associated with responses to EGCG in EpiDerm™ and NHEKs, we obtained gene expression profile data using microarrays of cells before (0 h) and 12 h after EGCG treatment at each cytotoxic dose (10 mg/mL for EpiDerm™ and 10 µg/mL for NHEKs). GO mapping was applied to the genes significantly altered by EGCG treatment. Expression levels of 2391 genes in EpiDerm™ and 3944 genes in NHEKs were altered as a result of the treatment, and 21 and 84 biological processes were identified, respectively (Tables 2 and 3).

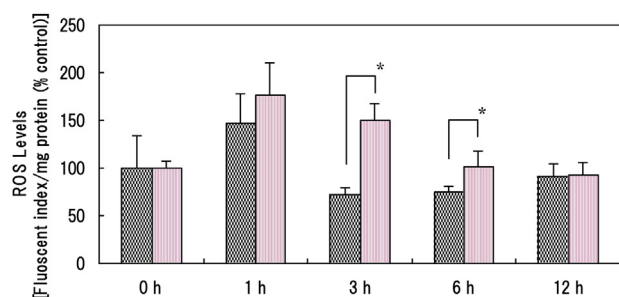


Fig. 8. Time course of reactive oxygen species (ROS) levels in EpiDerm™ and normal human epidermal keratinocytes (NHEKs) after the treatment with epigallocatechin gallate (EGCG). Doses of EGCG were 10 mg/mL for EpiDerm™ (checked bars) and 10 μ g/mL for NHEKs (striped bars). Error bars indicate standard deviation of triplicate experiments for each time point. * $P < 0.05$, ** $P < 0.01$: statistical significance between both models determined using the Student *t* test.

Genotoxicity-related responses were noted in NHEKs but not in EpiDerm™.

3.5. Cellular functions related to oxidative stress

ROS levels in EpiDerm™ and NHEKs were measured 0, 1, 3, 6, and 12 h after EGCG treatment as described above (Fig. 8). From 1 to 6 h after treatment, ROS levels in NHEKs were higher than those in EpiDerm™. The activities of the antioxidant enzymes CAT and GPx were measured in both models before (0 h) and 12 h after EGCG treatment. The CAT level in EpiDerm™ was 7.5-fold higher than that in NHEKs at 0 h and was increased after EGCG treatment in EpiDerm™ only (Fig. 9A). The GPx level in EpiDerm™ was also 6.7-fold higher than that in NHEKs at 0 h and increased in EpiDerm™ but decreased in NHEKs after EGCG treatment (Fig. 9B). Gene expression levels of *GCLC* (the first rate-limiting enzyme of glutathione synthesis), *CAT*, and *GPx* were measured using RT-PCR in both models at the same time points described above. *GCLC* expression was significantly upregulated after EGCG treatment (EpiDerm™, $P < 0.05$; NHEKs $P < 0.01$; Fig. 10A). *CAT* expression was downregulated in NHEKs but upregulated in EpiDerm™ after EGCG treatment ($P < 0.05$). *GPx1* expression was significantly upregulated in only EpiDerm™ after EGCG treatment ($P < 0.05$).

4. Discussion

In the present study, EpiDerm™ correctly identified *in vivo* genotoxins (MMC, MNU, and ENU) as positive and non-*in vivo* genotoxins (4-NP, EHD, EGCG, curcumin, and RES) as negative according to the RSMN assay protocol. These outcomes agreed with those of recent publications proposing that RSMN assay using EpiDerm™ is a promising *in vitro* follow-up for positive results in *in vitro* mammalian genotoxicity tests. However, NHEKs, a constituent of EpiDerm™, incorrectly identified three of four non-*in vivo* genotoxins evaluated.

Many suggestions have been made to improve the low predictivity of current *in vitro* genotoxicity tests. One of the suggestions is the p53 status of exposed cells. Cell lines that are not p53 competent or have a low proficiency for DNA repair are considered hypersensitive and not reflective of the behavior of normal mammalian cells in which DNA damage might be repaired or lead to apoptosis [14–17]. The working group at the 5th International Workshop on Genotoxicity Testing has suggested using human p53-competent cells (e.g., peripheral blood lymphocytes, TK6, and HepG2 cells) rather than rodent cell lines with impaired p53 function (e.g., L5178Y, V79, and Chinese hamster lung and ovary cells) for *in vitro* MN or chromosomal aberration tests [18].

However, our results with NHEKs, which are assumed to have normal p53 function, indicated that other features of EpiDerm™ contribute to its improved predictivity.

We used EGCG as a model of a non-*in vivo* genotoxin for further evaluation of the better predictivity of EpiDerm™. One possible feature related to the improvement was barrier function. The EpiDerm™ system is a multilayered, highly differentiated model of the human epidermis. The presence of a stratum corneum structure serves as a barrier, and the amount of test substance required for EpiDerm™ were much lower than those for NHEKs to show similar cytotoxicity. At the same time, the question of whether test substances reached target cells was raised. The results of our EGCG permeability analysis and RSMN assays by using an underdeveloped epidermal model, EpiDerm-201™, which has a partially cornified epidermal structure, indicated that the role of barrier function is limited.

The comparison of biological responses to EGCG treatment in EpiDerm™ and NHEKs with GO mapping of gene expression revealed unique features in both models. In EpiDerm™, biological processes related to cell differentiation (GO:0048513, GO:0048856, GO:0048731, and GO:0008544) and cell division (GO:0022402, GO:0007049, and GO:0022403) were altered after treatment. In addition, biological responses related to genotoxicity (response to DNA damage stimulus, GO:0006974; cellular response to DNA damage stimulus, GO:0034984; DNA repair, GO:0006281; DNA repair, GO:0006281; and cell cycle checkpoint, GO:0000075) were significantly altered in NHEKs but not in EpiDerm™. These responses substantiate the positive result of the RSMN assay in NHEKs. Biological processes were altered in NHEKs in greater numbers than those in EpiDerm™, which may indicate the extent of the disturbance of cellular homeostasis resulting from the treatment.

EGCG has antioxidant properties and prevents the genotoxic action of other chemicals [19]. However, it displays oxidative properties under *in vitro* conditions, especially at higher concentrations. Several reports have demonstrated that under *in vitro* culture conditions, EGCG or catechins, the family of chemicals to which EGCG belongs, generates H_2O_2 and gives a positive response in *in vitro* genotoxicity tests [20–22].

We further explored the oxidative properties of EGCG in the biological responses of both models. EGCG treatment increased ROS levels in both, indicating the induction of oxidative stress through EGCG. NHEKs were exposed to levels of ROS that were higher than those in EpiDerm™ from 1 to 6 h after treatment. Because the activities of the antioxidative enzymes CAT and GPx in EpiDerm™ were markedly higher than those in NHEKs and were further induced after EGCG treatment in EpiDerm™ but not in NHEKs, we concluded that EpiDerm™ eliminates ROS more effectively than NHEKs do. This phenomenon is also supported by observations of gene expression changes related to oxidative stress. Expression levels of *CAT* and *GPx* were significantly upregulated after EGCG treatment in EpiDerm™ but not in NHEKs. Furthermore, *GCLC* gene expression, which is known to be upregulated in response to oxidative stress, was significantly upregulated after EGCG treatment in NHEKs but not in EpiDerm™. These observations suggest that NHEKs have insufficient protective properties for ROS, which resulted in a positive response to EGCG treatment in the RSMN assay. By contrast, EpiDerm™ has antioxidative properties capable of eliminating the ROS formed after EGCG treatment under *in vitro* culture conditions, and therefore, gave negative results in the RSMN assay. In the living body, ROS such as H_2O_2 are formed everywhere; therefore, protective systems are highly developed [23]. In *in vivo* skin, an anti-property is induced in response to ROS generated from ultraviolet B radiation or oxidants [24,25]. Thus, EpiDerm™ is likely to keep its original properties *in vivo*, at least its antioxidative properties, whereas NHEKs are unlikely to do so. A key feature of EpiDerm™ is a 3-dimensional extracellular

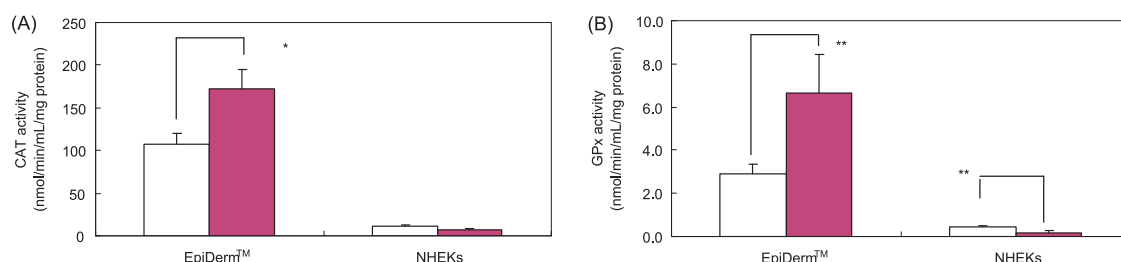


Fig. 9. Effect of epigallocatechin gallate (EGCG) treatment on (A) catalase (CAT) and (B) glutathione peroxidase (GPx) activities in EpiDerm™ and normal human epidermal keratinocytes (NHEKs). Doses of EGCG were 10 mg/mL for EpiDerm™ and 10 μ g/mL for NHEKs. White bars indicate levels in the concurrent control (0 h), and black bars indicate levels 12 h after treatment with EGCG. Error bars indicate standard deviation of triplicate experiments for each point. * P <0.05, ** P <0.01: statistical significance between concurrent control and EGCG treatment determined with the Student t test.

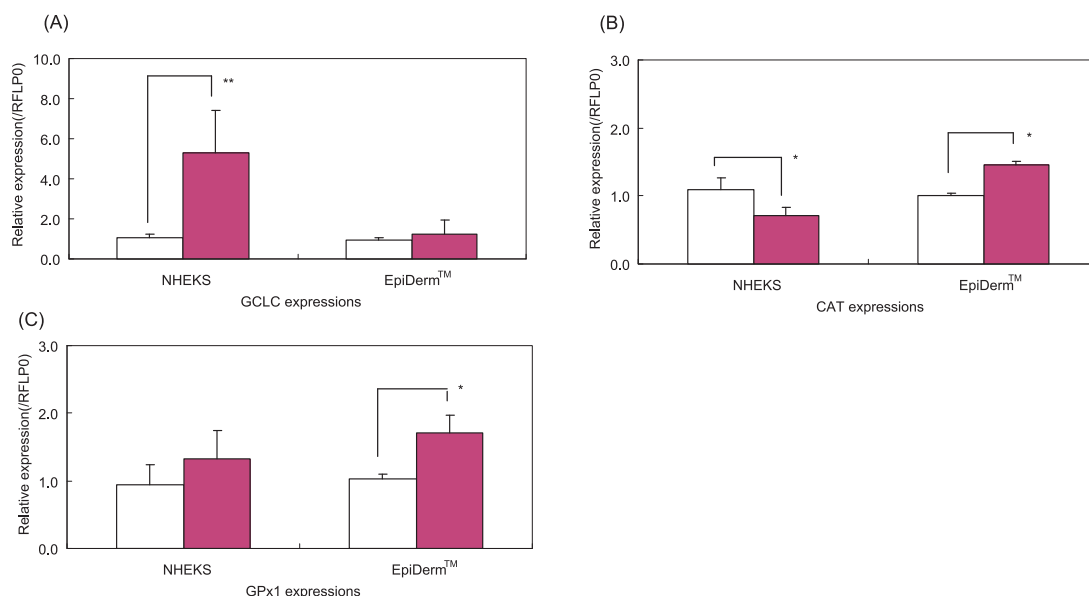


Fig. 10. Effect of epigallocatechin gallate (EGCG) treatment on messenger RNA expression of (A) glutamate-cysteine ligase, catalytic subunit (GCLC), (B) catalase (CAT), and (C) glutathione peroxidase 1 (GPx1) in EpiDerm™ and normal human epidermal keratinocytes (NHEKs). Doses of EGCG were 10 mg/mL for EpiDerm™ and 10 μ g/mL for NHEKs, respectively. White bars indicate levels in the concurrent control (0 h), and black bars indicate levels 12 h after EGCG treatment. These expression data were corrected using an internal standard. Error bars indicate standard deviation of triplicate experiments at each point. * P <0.05, ** P <0.01: statistical significance between concurrent control and EGCG treatment determined with the Student t test.

environment that mimics the environment in which cells routinely operate in vivo [26]. Although both models are derived from human skin, the more physiologically accurate culture conditions provide advantages for identifying in vivo genotoxins.

A large number of substances have been evaluated using RSMN assays with EpiDerm™. However, to be confident in the results of the RSMN assay as a follow-up to positive in vitro results, we believe that we need both to investigate further the mechanisms underlying these responses and to evaluate additional chemicals, especially those requiring metabolic activation to reveal their genotoxic potential.

In summary, in an evaluation of 8 chemicals through in vitro MN assay, the responses with EpiDerm™ conformed to those of in vivo MN assay, whereas those with NHEKs did not. Although further investigation using various model compounds is necessary, our investigation using EGCG suggests that EpiDerm™ displays antioxidant properties similar to those of the living body and therefore may give responses that reflect in vivo-like conditions more accurately than do the standard cell lines routinely used for in vitro genotoxicity tests.

Conflict of interest statement

None.

References

- [1] S. Pfuhler, A. Kirst, M.J. Aardema, N. Banduhn, C. Goebel, D. Araki, M. Costabel-Farkas, E. Dufour, R. Fautz, J. Harvey, N.J. Hewitt, J. Hibatalah, P. Carmichael, M. Macfarlane, K. Reisinger, J. Rowland, F. Schellau, A. Schepky, J. Scheel, A tiered approach to the use of alternatives to animal testing for the safety assessment of cosmetics: genotoxicity. A COLIPA analysis, *Mutat. Res. Regul. Toxicol. Pharmacol.* 57 (2010) 315–324.
- [2] D. Kirkland, M.J. Aardema, L. Henderson, Evaluation of the ability of a battery of three in vitro genotoxicity tests to discriminate rodent carcinogens and non-carcinogens: I. Sensitivity and relative predictivity, *Mutat. Res.* 584 (2005) 1–256.
- [3] D. Kirkland, S. Pfuhler, D. Tweats, M.J. Aardema, R. Corvi, F. Darroudi, A. Elhajoui, H. Glatt, P. Hastwell, M. Hayashi, P. Kasper, S. Kirchner, A. Lynch, D. Marzin, D. Maurici, J.R. Meunier, L. Muller, G. Nohynek, J. Parry, E. Parry, V. Thybaud, R. Tice, J.V. Benthem, P. Vanparys, P. White, How to reduce false positive results when understanding in vitro genotoxicity testing and thus avoid unnecessary follow-up animal tests: report of an ECVAM workshop, *Mutat. Res.* 628 (2007) 31–55.
- [4] R.D. Curren, G.C. Mun, D.P. Gibson, M.J. Aardema, Development of a method for assessing micronucleus induction in a 3D human skin model (EpiDerm™), *Mutat. Res.* 607 (2006) 192–204.
- [5] G.C. Mun, M.J. Aardema, T. Hu, B. Barnett, Y. Kaluzhny, M. Klausner, V. Karetzky, E.L. Dahl, R.D. Curren, Further development of the EpiDerm™ 3D reconstructed skin micronucleus (RSMN) assay: transferability and reproducibility, *Mutat. Res.* 673 (2009) 92–99.
- [6] T. Hu, Y. Kaluzhny, G.C. Mun, B. Barnett, V. Karetzky, N. Wilt, M. Klausner, R.D. Curren, M.J. Aardema, Intralaboratory and interlaboratory evaluation of the EpiDerm™ 3D human reconstructed skin micronucleus (RSMN) assay, *Mutat. Res.* 637 (2009) 100–108.

- [7] M.J. Aardema, B.C. Barnett, Z. Khambatta, K. Reisinger, C. Ouedraogo-Arras, B. Faquet, A.-C. Ginestet, C.C. Mun, E.L. Dahl, N.J. Hewitt, R.F. Corvi, R.D. Curren, International prevalidation studies of the EpiDerm™ 3D human reconstructed skin micronucleus (RSMN) assay: transferability and reproducibility, *Mutat. Res.* 7 (2010) 123–131.
- [8] E.L. Dahl, R.D. Curren, B.C. Barnett, Z. Khambatta, K. Reisinger, C. Ouedraogo, B. Faquet, A.-C. Ginestet, G. Mun, N.J. Hewitt, G. Carr, S. Pfuhler, M.J. Aardema, The reconstructed skin micronucleus assay (RSMN) in EpiDerm™: detailed protocol and harmonized scoring atlas, *Mutat. Res.* 720 (2011) 42–52.
- [9] M.J. Aardema, B.B. Barnett, C.C. Mun, E.L. Dahl, R.D. Curren, N.J. Hewitt, S. Pfuhler, Evaluation of chemicals requiring metabolic activation in the EpiDerm™ 3D human reconstructed skin micronucleus (RSMN) assay, *Mutat. Res.* 750 (2013) 40–49.
- [10] T. Hu, Z.S. Khambatta, P.J. Hayden, J. Bolmarcich, R.L. Binder, M.K. Robinson, G.J. Carr, J.P. Tiesman, B.B. Jarrold, R. Osborne, T.D. Reichling, S.T. Nemeth, M.J. Aardema, Xenobiotic metabolism gene expression in the EpiDerm™ in vitro 3D human epidermis models compared to human skin, *Toxicol. In Vitro* 24 (2010) 1450–1463.
- [11] T. Hu, R.E. Bailey, S.W. Morrall, M.J. Aardema, L.A. Stanley, J.A. Skare, Dermal penetration and metabolism of *p*-aminophenol and *p*-phenylenediamine: application of the EpiDerm™ human reconstructed epidermis model, *Toxicol. Lett.* 188 (2009) 119–129.
- [12] R.A. Isbrucher, J. Bausch, J.A. Edwards, E. Wolz, Safety studies on epigallocatechin gallate (EGCG) preparations. Part 1: Genotoxicity, *Food Chem. Toxicol.* 44 (2006) 626–635.
- [13] M.J. Lee, S. Prabhu, X. Meng, C. Li, C.S. Yang, An improved method for the determination of green and black tea polyphenols in biomatrices by high-performance liquid chromatography with coulometric array detection, *Anal. Biochem.* 279 (2000) 164–169.
- [14] W. Chaung, L.J. Mi, R.J. Boorstein, The p53 states of Chinese hamster V79 cells frequency used for studies of DNA damage and DNA repair, *Nucleic Acid Res.* 25 (1997) 992–994.
- [15] H. Oka, K. Ikeda, H. Yoshimura, A. Ohuchida, M. Honma, Relationship between p53 states and 5-fluorouracil sensitivity in 3 cell lines, *Mutat. Res.* 606 (2006) 52–60.
- [16] D. Kirkland, S. Pfuhler, D. Tweats, M.J. Aardema, R. Corvi, F. Darroudi, A. Elhajouji, H. Glatt, P. Hastwell, M. Hayashi, P. Kasper, S. Kirchner, A. Lynch, D. Marzin, D. Maurici, J.R. Meunier, L. Muller, G. Nohynek, J. Parry, E. Parry, V. Thybaud, R. Tice, J.V. Benthem, P. Vanparys, P. White, How to reduce false positive results when understanding in vitro genotoxicity testing and thus avoid unnecessary follow-up animal tests: report of an ECVAM workshop, *Mutat. Res.* 628 (2007) 31–55.
- [17] P. Fowler, J. Young, L. Jeffrey, T. Hand, K. Smith, D. Kirkland, P. Carmichael, S. Pfuhler, Reduction of misleading (“False”) positive results in mammalian cell genotoxicity assays. I. Choice of cell type, *Mutat. Res.* 742 (2012) 11–25.
- [18] S. Pfuhler, M. Fellows, J. Van Benthem, R. Corvi, R.D. Curren, K. Dearfield, P. Fowler, R. Frötschl, A. Elhajouji, L.L. Hégarat, T. Kasamatsu, H. Kojima, G. Ouedraogo, A. Scott, G. Speit, In vitro genotoxicity test approaches with better predictivity: summary of an IWGT workshop, *Mutat. Res. Genet. Toxicol. Environ. Mutagen.* 723 (2011) 101–107.
- [19] C.A. Rice-Evans, N.J. Miller, G. Paganga, Structure-antioxidant activity relationships of flavonoids and phenolic acids, *Free Radical Biol. Med.* 20 (1996) 933–956.
- [20] A. Sugisawa, K. Umegaki, Physiological concentrations of (–)-epigallocatechin-3-O-gallate (EGCG) prevent chromosomal damage induced by reactive oxygen species in WIL2-NS cells, *J. Nutr.* 132 (2002) 1836–1839.
- [21] M.K. Johnson, G. Loo, Effects of epigallocatechin gallate and quercetin on oxidative damage to cellular DNA, *Mutat. Res.* 459 (2000) 211–218.
- [22] A. Takumi-Kobayashi, R. Ogura, O. Morita, N. Nishiyama, T. Kasamatsu, Involvement of hydrogen peroxide in chromosomal aberrations induced by green tea catechins in vitro and implications for risk assessment, *Mutat. Res.* 657 (2008) 13–18.
- [23] S. Hsu, Green tea and the skin, *J. Am. Acad. Dermatol.* 52 (2005) 1049–1059.
- [24] F.R. Brigelius, Glutathione peroxidases and redox-regulated transcription factors, *Biol. Chem.* 387 (2006) 1329–1335.
- [25] M. Meloni, J.F. Nicolay, Dynamic monitoring of glutathione redox status in UV-B irradiated reconstituted epidermis: effect of antioxidant activity on skin homeostasis, *Toxicol. In Vitro* 17 (2003) 609–613.
- [26] A.T. Grazul-Bilska, J.J. Bilski, D.A. Redmer, K.M. Abdullah, A. Abdullah, Antioxidant capacity of 3D human skin EpiDerm™ model: effects of skin moisturizers, *Int. J. Cosmet. Sci.* 31 (2009) 201–208.